Open access • Journal Article • DOI:10.1063/1.1776531

On the dynamics of self-sustained one-dimensional detonations: A numerical study in the shock-attached frame — Source link

Aslan R. Kasimov, D. Scott Stewart

Institutions: University of Illinois at Urbana–Champaign

Published on: 10 Aug 2004 - Physics of Fluids (American Institute of Physics)

Topics: Boundary value problem, Euler equations, Detonation, Shock wave and Boundary (topology)

On the dynamics of self-sustained one-dimensional detonations: A numerical study in the shock-attached frame

Aslan R. Kasimov and D. Scott Stewart[a)]
Department of Theoretical and Applied Mechanics, University of Illinois at Urbana-Champaign, Urbana, Illinois 61801

(Received 4 December 2003; accepted 28 May 2004; published online 10 August 2004)

In this work we investigate the dynamics of self-sustained detonation waves that have an embedded information boundary such that the dynamics is influenced only by a finite region adjacent to the lead shock. We introduce the boundary of such a domain, which is shown to be the separatrix of the forward characteristic lines, as a generalization of the concept of a sonic locus to unsteady detonations. The concept plays a fundamental role both in steady detonations and in theories of much more frequently observed unsteady detonations. The definition has a precise mathematical form from which its relationship to known theories of detonation stability and nonlinear dynamics can be clearly identified. With a new numerical algorithm for integration of reactive Euler equations in a shock-attached frame, that we have also developed, we demonstrate the main properties of the unsteady sonic locus, such as its role as an information boundary. In addition, we introduce the so-called "nonreflecting" boundary condition at the far end of the computational domain in order to minimize the influence of the spurious reflected waves. © *2004 American Institute of Physics*. [DOI: 10.1063/1.1776531]

I. INTRODUCTION

A self-sustained detonation wave is defined as a detonation that once initiated does not require any external support to sustain its subsequent evolution. Such detonations propagate by means of the interaction of the lead shock with the following reaction zone only. This is unlike overdriven detonations which require additional external support, such as a piston, to maintain the detonation structure at its nominal speed. Self-sustained detonations are of great theoretical and practical interest precisely because of the property of their autonomous dynamics and because they can produce useful work on their own without continuous external energy input. Existing theoretical and numerical studies have dealt principally with overdriven detonations because of their simpler mathematical formulation.

The steady planar Chapman–Jouguet (CJ) detonation is the classical example of a self-sustained detonation. The distinct feature of the CJ detonation is the existence of a sonic point at the end of the reaction zone. We emphasize two fundamental properties of the sonic point. First, the condition of local sonicity, namely that the Mach number defined in terms of the particle speed relative to the lead shock is unity at the sonic point. In one dimension, enforcement of a sonic state at the end of the reaction zone as a pointwise condition (i.e., a boundary condition) serves as a closure equation that determines the detonation speed for a given explosive mixture. A second fundamental property is that the flow between the lead shock and the sonic locus is acoustically isolated from the far-field flow, that is the sonic locus is an information boundary such that acoustic information on the downstream side of this boundary cannot penetrate into the detonation reaction zone. The second property is important in a generalization of the sonic point to unsteady detonations. The lack of understanding of the nature of the confinement of self-sustained detonation (also sometimes referred to as "freely propagating" detonation) has been a source of tremendous confusion in the subject and a satisfactory resolution has been a long-standing open problem in detonation theory.

In this work we define a sonic locus in an unsteady detonation as a separatrix of the family of forward characteristics. On the upstream side of the separatrix, the characteristics flow into the shock in a finite time, while on the downstream side, they flow away from the shock. In this view the sonic locus (in one dimension) is a point on a particular forward space–time characteristics. It agrees entirely with the standard definition of the sonic locus when the flow is steady. The definition can be put in precise mathematical terms. By means of a new numerical approach that we have developed for this study, we demonstrate the physical properties of the unsteady sonic locus by computing a pulsating detonation wave with a finite reaction zone. By placing a variety of different initial states behind the sonic locus, we demonstrate that the separatrix is an information boundary. We show that, as long as the flow within the reaction zone evolves smoothly, the separatrix exists and indeed acoustically isolates the reaction zone from the subsequent flow.

The present findings about the nature of the sonic locus in unsteady detonations have important implications for theories of detonation stability and nonlinear dynamics. We show that the conditions that must be satisfied at the sonic locus have a direct relationship to radiation conditions of detonation stability theory (see, e.g., Ref. 8), as well as con-

a)Author to whom correspondence should be addressed. Electronic mail: dss@uiuc.edu

ditions that have been used in nonlinear theories of detonation shock dynamics.[9]

The computation of detonation dynamics is difficult due to the need for tremendous resolution and because there are many sources of noise and error from the numerics, and first-order error from the lead shock, in particular. Therefore we have developed a highly accurate numerical method based on a transformation to a frame attached to the lead shock. In this approach, the lead shock is treated as a boundary instead of being tracked, or captured. This allows us to carry out simulations of the dynamics of self-sustained detonations, in particular, and enables direct comparisons with theories cast in terms of the detonation shock speed and its derivatives. It is fair to say that despite the number of high-resolution simulations carried out by various researchers over recent years (see, e.g., Refs. 1–6), a definitive conclusion as to what it means to have an adequate resolution has yet to be made, even for one-dimensional detonations. Close to the stability boundary when detonation propagates in the form of regular pulsations, one can obtain a converged solution provided sufficient resolution is used and the computational domain size is sufficiently large. But far from the stability boundary when detonation propagation is irregular with seemingly chaotic pulsations, interpretation of the calculations is not straightforward. There can be a strong dependence of the computed solution on the grid size and the size of the computational domain as well as on the numerical algorithm. As simulations show, for a wide range of system parameters, complex multimode or chaotic solutions are much more common than regular ones. Clearly, understanding the nature of such complex solutions is of great interest. In order to attain such understanding one needs to have reliable tools in hand. If the problem is addressed by means of a numerical integration of governing equations, then the effects of all possible sources of numerical error must be minimized, and a high-resolution numerical algorithm must be used. In terms of numerical algorithms for solving Euler equations, a variety of highly accurate discretization schemes are available presently. Still an accurate treatment of detonation shocks is a problem in schemes that capture or track the shock because of inherent oscillations present near the shock that preclude accurate calculations of the shock position, speed, and hence the shock pressure. Inaccurate (first order) calculation of the lead shock generates errors in the pressure and density (and hence the temperature) and in turn generate accuracy errors in the initial chemical reaction rate at the shock that in turn propagate into the reaction zone.

In addition to the errors that have their origin in discretization and shock tracking, the rear boundary conditions can also be a source of error. In all previous studies the issue of the far-field boundary condition has been avoided by using very large computational domains, sometimes employing adaptive mesh refinement, and setting the "outflow" or "soft" boundary condition. In outflow boundary conditions, one extrapolates the flow variables from the interior side of the numerical boundary into the ghost points, thus imposing zero gradients of the flow variables (see, e.g., Refs. 4 and 5). The outflow boundary condition is not based on physical reasoning and is used because it does not produce any *visible* reflections and because it is efficient and simple to implement when the flow is supersonic. As we will show below, the outflow condition does produce spurious reflected waves. Various other conditions have also been used, such as continuous gradients, fixed pressure,[2,6] etc., again these are all nonphysical, because strong outgoing oscillating waves generated by the pulsating detonation reaction zone do change both the gradients of flow variables and pressure at the outflow boundary.

In order to contribute to proper theoretical understanding of detonation dynamics, numerically generated results must be unambiguous and independent of discretization schemes and unphysical effects of domain size and boundary conditions. That said, it must be realized that such a requirement may not be achievable in certain cases, one such being the computation of chaotic dynamics. If a detonation wave is chaotic by its nature, it implies exponential sensitivity to initial conditions; that is, small differences in initial conditions will be amplified over time leading to completely different long-time solutions. It may be possible to demonstrate the existence of "chaos" in such cases, but nearly impossible to compute a "converged" solution in the conventional sense. In such cases, the strong grid dependence will be intrinsic to the computed dynamics and thus higher resolutions would not appear to produce a converged solution. At the time of this writing, careful analysis of such chaotic solutions is absent in the literature.

In order to address the issues related to the errors in determining shock location and speed as well as to the effects of outflow boundary conditions, we employ a simple to implement method for calculation of the one-dimensional detonation waves in a frame of reference attached to the lead shock front and have implemented a dynamic rear boundary condition that reduces the spurious reflections at the outflow boundary. High accuracy, simplicity of implementation, and convenience in analyzing the results makes our approach appealing as it can be used as a tool for careful comparisons of high-resolution simulations with theoretical results. Detonation theories are often posed in the shock-attached frame. For example, the entire theory of detonation instability is posed in terms of shock-attached coordinates, see, e.g., Refs. 7 and 8. Similarly, the theory of detonation shock dynamics, which is a weak disturbance theory is also formulated in shock-attached coordinates, see, e.g., Ref. 9.

For the region behind the shock, we use a standard shock-capturing algorithm but posed in the shock-attached frame. As a consequence of the coordinate transformation to the lead shock, the shock speed, $D(t)$, enters the governing equations explicitly as an unknown and must be calculated at each time step. We do this by local method of characteristics integration of the equation for the forward characteristic near the shock, combined with the application of the shock relations to determine $D(t)$. The method eliminates the ambiguities and inaccuracies in the computation of the lead shock speed. Computation in the shock-attached frame gives us the luxury of placing tremendously large number of points in the reaction zone if we so desire. We do not have to *a posteriori* place or filter the shock location, rather it is a boundary set at the origin at all times.

The study and testing of nonreflecting outflow boundary conditions have been a subject of interest for computations of compressible flows and turbulent flows. For a general discussion, the reader is referred to the papers by Thompson[13] and by Poinsot and Lele.[14] In this paper, we formulate a nonreflecting boundary condition in terms of the method of characteristics similar to the earlier works and give the implementation details. We tested this boundary condition on the problem of an acoustic pulse that is propagating in a uniformly shocked region behind a shock. We demonstrate that our boundary condition reduces the acoustic reflections by an order of magnitude compared to the "soft" boundary condition. We also demonstrate that reflecting the outflow boundary condition can noticeably affect the detonation dynamics.

For the purpose of validation and comparison, we have tested our method with an example of a shock overtaking another shock in an inert medium and have computed several cases of detonation that have also been previously published.[2,5,6] Our calculations agree with predictions of linear stability analysis and with known results for detonations that are known to have a converged solution namely for low-frequency pulsating detonations. But we found that for one, still controversial, case of a detonation wave that undergoes initial decay with subsequent reignition, the spurious errors that are always present near the shock at the start of computations in traditional shock-capturing methods, play a significant role in the initial evolution of the wave. Namely, the shock-based errors are responsible for the formation of strong high-frequency pulsations before the reaction front starts to decouple from the lead shock. Such oscillations have been shown in Ref. 4 to be responsible for the appearance of unburnt pockets of fuel and an irregular grid-dependent reignition process. For exactly the same problem, we show that the initial errors are significantly reduced in magnitude, more so with higher resolutions, and we do not observe the growth of high-frequency oscillations. The result is that the dynamics is governed by the nonlinear instability and dominated by the low-frequency mode, quite similar to that of the original work of He and Lee;[6] therefore, the subsequent reignition process is also much more regular that is localized explosions due to the unburnt pockets are absent, as opposed to the results of Refs. 4 and 5, where such explosions were observed. We observe the high-frequency oscillations only if an artificial initial perturbation is introduced behind the shock. Even extremely high resolution simulations that used 533 grid points per half-reaction length led to the same regular dynamics with no high-frequency oscillations if no initial perturbations were present.

In order to clarify the physical role played by the unsteady sonic locus (the acoustic information boundary for the lead shock) in self-sustained detonations we carried out a series of simulations of an initially steady CJ detonation with a reaction zone of finite thickness. We used an Arrhenius rate law with depletion factor of $\nu=0.9$ which makes the reaction zone finite. The location of the sonic locus for the steady detonation coincides with the end of the reaction zone. By demonstration, we show that the information boundary exists and can be given a precise meaning, namely that it is a separatrix of the family of forward characteristic lines that delineates the characteristics that reach the lead shock in finite time and those that leave to infinity. We show that if the postsonic state remains sufficiently smooth then the detonation dynamics is not influenced by the processes behind the separatrix and is determined entirely by the finite region between the lead shock and the separatrix. The general version of this argument is simply based on a domain of influence considerations for hyperbolic partial differential equations.

The present study considers a mixture with an ideal equation of state, that undergoes single-step irreversible chemical reaction. With straightforward modifications this work can be generalized for one-dimensional detonations with multiple-step chemistry and/or nonideal equation of state.

II. GOVERNING EQUATIONS IN THE SHOCK-ATTACHED FRAME

The reactive Euler equations are rewritten in the shock-attached frame, (x,t), where

$$x = x^l - \int_0^{t^l} D dt, \quad t = t^l, \tag{1}$$

and superscript l denotes the laboratory frame. We consider the wave moving from left to right, hence $x<0$ is the region behind the lead shock. The governing equations in conservative form are as follows:

$$\frac{\partial \mathbf{y}}{\partial t} + \frac{\partial}{\partial x}(\mathbf{F} - D\mathbf{y}) = \mathbf{S}, \tag{2}$$

where

$$\mathbf{y} = \begin{pmatrix} \rho \\ \rho u \\ \rho E_T \\ \rho \gamma \end{pmatrix}, \quad \mathbf{S} = \begin{pmatrix} 0 \\ 0 \\ 0 \\ \rho \omega \end{pmatrix},$$

$$\mathbf{F} = \begin{pmatrix} \rho u \\ \rho + \rho u^2 \\ \rho u (E_T + pv) \\ \rho u \lambda \end{pmatrix}. \tag{3}$$

Note that $u=U+D(t)$ here is the particle velocity in the *laboratory* frame, $U<0$ is the particle velocity in the *shock-attached* frame, D is the shock speed, $E_T=e+u^2/2$ is the total specific energy, Q is the heat release, $e=pv/(\gamma-1)-\lambda Q$ is the specific internal energy of the ideal explosive mixture, $\omega=k(1-\lambda)^\nu \exp(-E/RT)$ is the Arrhenius reaction rate with activation energy E, reaction order ν, and pre-exponent k, R is the universal gas constant, and T is temperature.

The exact Rankine–Hugoniot conditions applied at the lead shock are

$$\rho_0 D = \rho_s U_s, \tag{4}$$

$$\rho_0 + \rho_0 D^2 = p_s + \rho_s U^2, \tag{5}$$

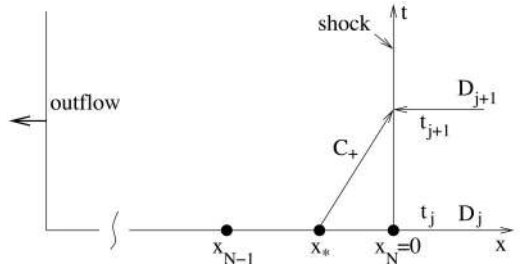

FIG. 1. Integration on the C_+ characteristic from $x=x_*$ near the shock to the location of the shock.

$$\frac{\gamma}{\gamma-1}\frac{p_0}{\rho_0}+\frac{D^2}{2}=\frac{\gamma}{\gamma-1}\frac{p_s}{\rho_s}+\frac{U_s^2}{2}. \tag{6}$$

The lead shock speed, D, enters the governing equations explicitly in contrast to the traditional formulations that used shock-capturing methods in which D is determined by the solution generated by the conservative, shock-capturing numerical scheme. In the shock-attached formulation, D must be calculated explicitly by some other means.

From now on we use the tilde to denote a dimensional quantity. The governing equations are rescaled as follows. Pressure and density are scaled with respect to their initial values, $\tilde{p}_0$ and $\tilde{\rho}_0$ in the fresh mixture, the velocity is scaled as $\tilde{u}=\sqrt{\tilde{p}_0/\tilde{\rho}_0}$, the length scale is that of the half-reaction length, $\tilde{l}_{1/2}$, and the time scale is $\tilde{t}_{1/2}=\tilde{l}_{1/2}/\tilde{u}$. In these scales the governing equations retain their form.

III. CALCULATION OF THE SHOCK SPEED

In order to integrate the governing system of equations, Eq. (2), one needs to be able to calculate the shock speed, D, at each time step. While the flow variables can be advanced in time by any finite-difference scheme, the front speed calculation must be based on an independent algorithm. We update the speed by integrating the governing equation on the C_+ characteristic near the shock from its location at $t=t_j$ to the location of the shock, Fig. 1, over the time interval Δt, given by the Courant condition. The exact Rankine–Hugoniot conditions (4)–(6) are imposed at the shock located at the right boundary of the computational domain, $x=0$. All the state variables at the shock are extended into the ghost points ahead of the shock, $x>0$. This procedure is somewhat similar to what is traditionally done in shock-tracking methods (see, e.g., Ref. 10), but in our approach we do not track the shock as a moving boundary, but rather it is always fixed at $x=0$.

The governing equations written in characteristic form on the C_+ characteristics are

$$\frac{dp}{dt}+\rho c\frac{du}{dt}-(\gamma-1)Q\rho\omega=0, \tag{7}$$

and

$$\frac{dx}{dt}=c+u-D. \tag{8}$$

In discretized form with first order differencing of the derivatives and semi-implicit treatment of ρc and implicit treatment of the reaction term, we obtain the following equations:

$$p_{j+1}-p_*+0.5[(\rho c)_*+(\rho c)_{j+1}](u_{j+1}-u_*) -(\gamma-1)Q\rho_{j+1}\omega_{j+1}\Delta t=0, \tag{9}$$

$$-x_*=(c_*+u_*-D_*)\Delta t. \tag{10}$$

The state at time t_j is considered known. The unknowns here are the point $x=x_*$ of the origin of the C_+ characteristic from time t_j to time t_{j+1}, and the front speed D_{j+1} at $t=t_{j+1}$. All the state variables at t_{j+1} that appear in Eq. (9), are explicit functions of D_{j+1} by means of the Rankine–Hugoniot conditions (4)–(6). The variables at $x=x_*$ can be calculated in terms of the known grid values at x_N,x_{N-1}, etc., by interpolation (N is the number of grid points). We use a linear interpolation in all calculations below. For example,

$$p_*=p_N-\frac{x_*}{\Delta x}(p_{N-1}-p_N), \tag{11}$$

where Δx is a fixed grid size.

The Rankine–Hugoniot relations (4)–(6) can be recast in terms of the detonation Mach number, $M_{j+1}=D_{j+1}/c_0$, to eliminate all variables at t_{j+1} in favor of M_{j+1} as follows:

$$\frac{p_{j+1}}{p_0}=\frac{2\gamma}{\gamma+1}M_{j+1}^2-\frac{\gamma-1}{\gamma+1}, \tag{12}$$

$$\frac{\rho_{j+1}}{\rho_0}=\frac{(\gamma+1)M_{j+1}^2}{2+(\gamma-1)M_{j+1}^2}, \tag{13}$$

$$\frac{u_{j+1}}{c_0}=\frac{U_{j+1}+D}{c_0}=\frac{2}{\gamma+1}\frac{M_{j+1}^2-1}{M_{j+1}}. \tag{14}$$

Substitution of these relations together with the linear interpolations such as Eq. (11) into Eqs. (10) and (9) results in a system of two nonlinear algebraic equations for x_* and M_{j+1}. The latter can be solved with any standard root solver.

Once we find D_{j+1} by the above procedure, we can then integrate the governing Eq. (2) to determine the entire flow behind the shock at the next time level, t_{j+1}. We use the UNO2 (Uniformly Non-Oscillatory) scheme,[11] of second-order spatial accuracy and third-order Runge–Kutta method for temporal integration, based on a numerical code developed in Ref. 12. We have tested a variety of ENO-type schemes and found that the most accurate solution a provided with a fifth-order WENO, but UNO2 was only slightly less accurate while faster than WENO by about 25%. For this reason we used UNO2 in all of the following calculations.

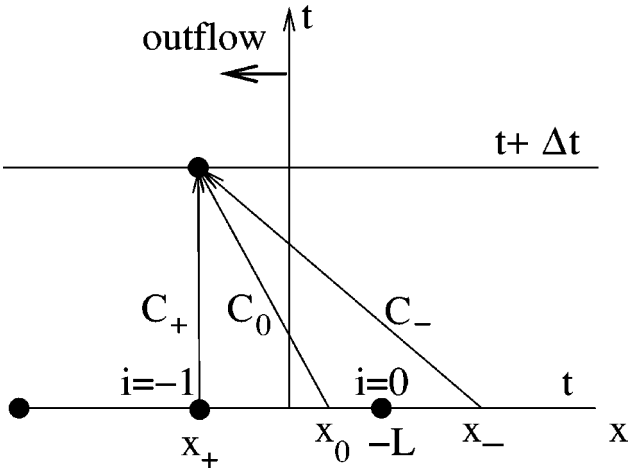

FIG. 2. Characteristics at the subsonic outflow at the left boundary for nonreflecting boundary condition: C_-: $dx/dt=u-c$, C_o: $dx/dt=u$, C_+: $dx/dt=u+c$.

IV. FAR-FIELD NONREFLECTING BOUNDARY CONDITION

At the far-left end of the computational domain, $x=-L$, we apply the nonreflecting boundary condition. For a subsonic outflow, the forward characteristics C_+ carries information from the outside region into the interior domain. Therefore, one boundary condition must be provided that specifies the details of the flow in the exterior. If no waves are assumed to enter the domain from outside, the boundary condition must reflect this fact. The appropriate condition is then the nonreflecting boundary condition (NRBC).

We formulate the nonreflecting condition in terms of the values at the ghost points, that is we have to update the ghost points at each time step so that the incoming wave is suppressed. The latter is accomplished by the method of characteristics as follows. The state variables in the ghost points will change in time due to the waves carried along the C_- and C_0 characteristics from the interior and the wave along the C_+ characteristic from outside, Fig. 2. But if the latter is assumed not to propagate into the interior domain, the C_+ characteristics cannot have a positive slope. And since the flow is assumed to be subsonic (or sonic), the direction must be vertical as shown in Fig. 2. The basic physics behind NRBC is that there should be no incoming wave. It means that the amplitude of any incoming wave does not change in space, that is the wave does not propagate. It can be shown (see, e.g., Ref. 14), that the equation for the C_+ characteristics is an amplitude equation for the incoming wave. Constancy of the amplitude means that the origin of the C_+ characteristics can be placed at any spatial position at the previous time level. All such characteristics will carry a wave of the same amplitude. The choice we have made is the simplest one, that is, we place the origin exactly at the boundary of the computational domain.

Thus we write the governing equations in characteristic form and generate the following discretized set of equations that are used to calculate the updated state at the ghost point $i=-1$:

$$J_0\colon\ p_+ - p_0 - c_0^2(\rho_+ - \rho_0) = 0, \tag{15}$$

$$C_0\colon\ x_+ - x_0 = \Delta t(u_0 - D), \tag{16}$$

$$J_-\colon\ p_+ - p_- - \rho_- c_-(u_+ - u_-) = 0, \tag{17}$$

$$C_-\colon\ x_+ - x_- = \Delta t(u_- - D - c_-), \tag{18}$$

$$J_+\colon\ p_+ - p_+^0 + \rho_+^0 c_+^0(u_+ - u_+^0) = 0, \tag{19}$$

$$C_+\colon\ x_+ = -L - \Delta x. \tag{20}$$

Here x_+, x_-, x_0 are the values of the intersections of the characteristic lines with x-axis at the current time level t. Except for p_+, ρ_+, and u_+, which are evaluated at $t=t+\Delta t$, all other variables are evaluated at time t at corresponding values of x. The unknowns in the above system are x_0, x_- and p_+, ρ_+, u_+. The superscript 0 indicates the state at x_+ at time t. Linear interpolation is used to calculate the interior states in terms of the known grid values. Once we find p_+, ρ_+, u_+ at $i=-1$, we extend them into the remaining ghost points. If the outflow is supersonic, then the extrapolation can be used to find the ghost point values (which we have done below) or the above system can be integrated on all three characteristics, which now carry information from the interior only.

It is interesting to note the close relationship between the non-reflecting boundary condition, which is expressed by Eq. (19) in the above system, and the radiation condition used in the linear stability theory.[8] In fact, the two are exactly the same as they both express the condition that there is no radiation from the outflow boundary. Linearization of Eq. (19) does indeed yield the one-dimensional radiation condition of the linear stability theory of detonation.

We tested the boundary condition on a problem of an acoustic pulse propagating downstream behind a steady shock. At time $t=0$, we have a uniform state of length $L=10$ behind a shock of Mach number $M=6$ and a superimposed acoustic perturbation of density $\rho'=\varepsilon \exp[-2(x+0.5L)^2]$, pressure $p'=c_0^2\rho'$, and velocity $u'=-p'/\rho_0 c_0$; here $\varepsilon=10^{-4}$, the base-state density $\rho_0=10.33$, pressure $p_0=39.18$, sound speed $c_0=2.13$, specific heat ratio $\gamma=1.2$. The perturbation propagates downstream and partially reflects off the left boundary. Figure 3 shows the results for two resolutions, $N=100$ and $N=200$ points in the computational domain at time $t=3.07$. For $N=100$ and with the outflow boundary condition (RBC, which is the soft boundary condition that extrapolates values from the interior to the ghost points), the reflected wave is a step-like decrease of pressure of amplitude of about $\delta p=6\cdot 10^{-7}$ which remains at this level as long as no other perturbation changes it. The new boundary condition produces a smaller reflection of amplitude of about $\delta p=7\cdot 10^{-8}$ or less which dissipates as it propagates to the right and there is no sustained pressure increase or decrease behind the reflected wave. For a higher resolution of $N=200$ the RBC produces a reflection of a smaller amplitude, but now it is a step-like increase in pressure. The reflection produced by the nonreflecting boundary condition (NRBC) is similar to the $N=100$ case, but is of smaller amplitude.

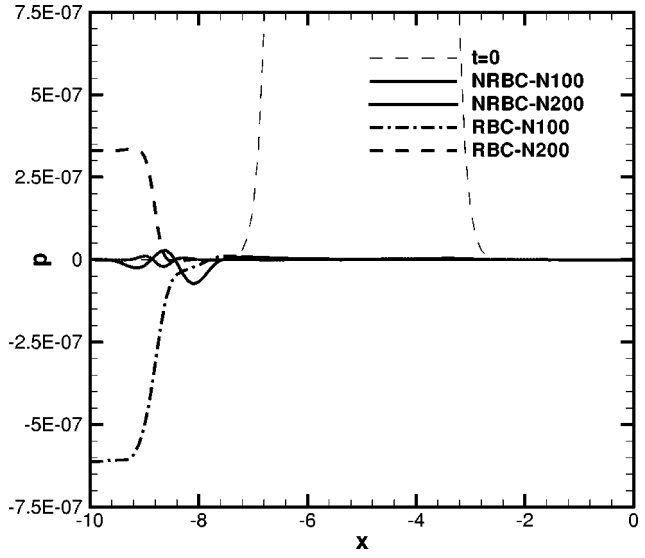

FIG. 3. Propagation of an acoustic pulse behind a shock: initial pressure perturbation profile (thin dashed line, only bottom part of the profile is shown since the maximum of the initial profile is $4.5\cdot10^{-4}$) and spurious reflections after the pulse leaves the domain, for nonreflecting (NRBC) and soft reflecting (RBC) boundary conditions at resolutions of $N=100$ and $N=200$.

V. RESULTS

The main purpose of the study is to gain an understanding of the dynamics of self-sustained detonations and the nature of their rear confinement, as discussed in Sec. V C. But first we demonstrate that the numerical approach in the shock-attached frame described in the last section produces highly accurate results by computing: (a) the interaction of two shock waves, one overtaking the other, and (b) the low-frequency pulsating detonation. The problem (a) of shock interaction has an analytic solution first obtained by von Neumann,[15] which is used to validate the code. In the case (b) of a pulsating detonation with simple-depletion Arrhenius kinetics, we perform several calculations near the stability boundary, predicted by the linear stability theory,[8] in order to capture the stability threshold and periods of pulsations. In addition, we also perform several calculations far from the stability boundary in order to gain insight into the behavior of detonation when the reaction front detaches significantly from the lead shock.

A. A shock overtaking another shock

The details of von Neumann's analytical solution can also be found in Ref. 16. For the sake of completeness, we reproduce here the basic idea of the solution. The schematics of the interaction in the $x-t$ plane is shown in Fig. 4, while Fig. 5 shows the initial pressure profiles (not to scale) and the speeds of the two shocks. The trailing shock S_2, propagating with speed $D_2=12$ in the lab frame overtakes the leading shock S_1 of speed $D_1=6$ with the new shock S_3 of speed D_3, a rarefaction wave R, and a contact discontinuity C forming as a result of the interaction. The computational domain is fixed at the leading shock front at all times.

The analytical solution of this problem is conveniently

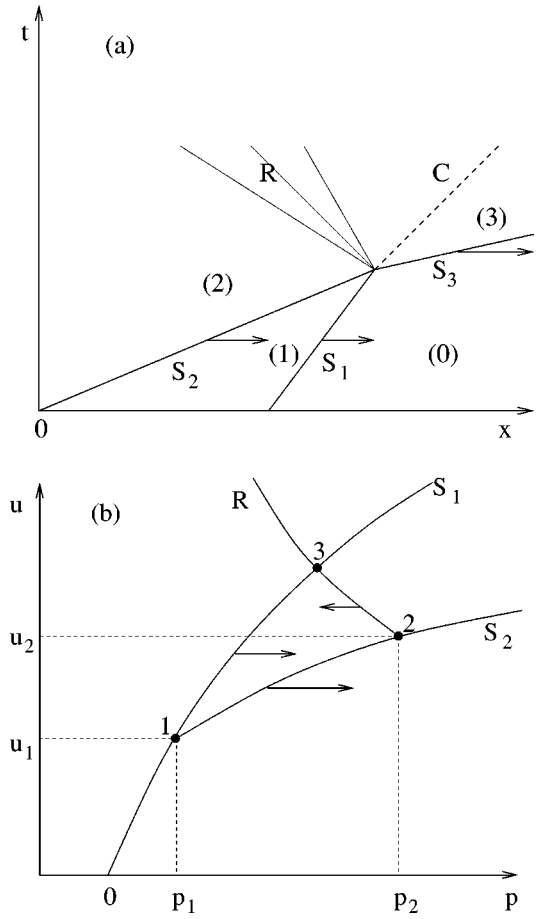

FIG. 4. Schematic of a shock-overtaking-a-shock interaction: (a) $x-t$ diagram of the interaction and (b) $p-u$ diagram of the interaction.

obtained with the help of the $p-u$ diagram shown in Fig. 4(b). The initial state is denoted by (0), the state behind the first shock is (1), that behind the second shock is (2), and the state behind the transmitted shock is (3). The goal is to find the state (3). As we can see from the figure, it is found as the intersection point of the shock curve S_1 and the rarefaction curve R. The latter originates at point (2), the state behind the second shock, since it is the state into which the rarefaction wave propagates.

The equations of S_1 and R are as follows:

$$S_1:\ u=(u-p_0)\sqrt{\frac{2/\rho_0}{(\gamma-1)p_0+(\gamma+1)p}},$$

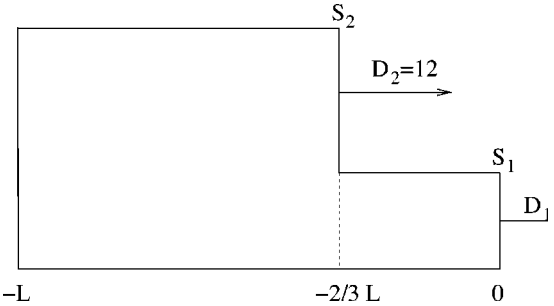

FIG. 5. Schematic of a shock-overtaking-a-shock interaction with initial condition as used in the calculations below.

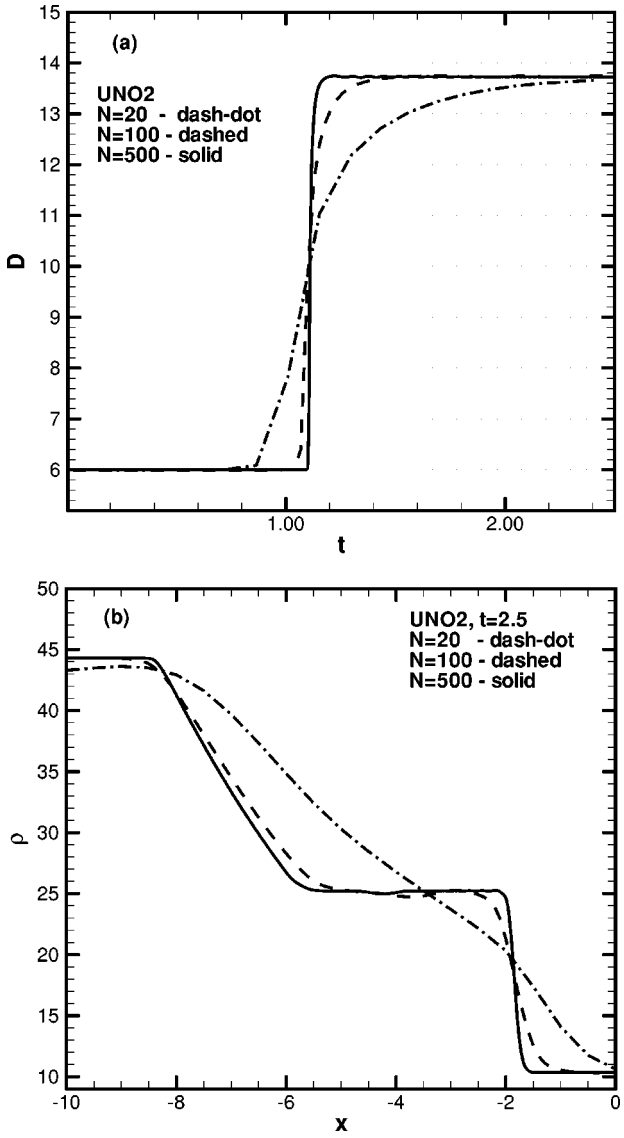

FIG. 6. Numerically calculated speed of the lead-shock as a function of time for three levels of resolution: (b) Density profiles at various resolutions at time $t=2.5$.

$$R\text{: } p = p_2\left(1 - \frac{\gamma-1}{2}\frac{u-u_2}{c_2}\right)^{2\gamma/(\gamma-1)}.$$

The solution of these equations gives the pressure at state (3) and hence the shock speed D_3. The point (2) in these equations is found by application of the Rankine–Hugoniot conditions first for state (1) in front of the shock S_2, and then for the state (2) behind it.

Figure 6 shows the numerically calculated shock speed as a function of time for three levels of resolution, $N=20, 100$, and 500 grid points in the domain of length $L=10$. We can see that the shock speed after the interaction is calculated with very high accuracy even for the lowest resolution of 20 points. For $N=500$ points, the numerically found shock speed after the interaction is $D_{\text{num}}=13.727$ which, to this accuracy, is the same as the theoretical value. The main difference between the curves is in the width of the transition region, which in theory must be zero, but is smeared in the calculations due to the smearing of the impinging shock S_2 by the spatial discretization scheme.

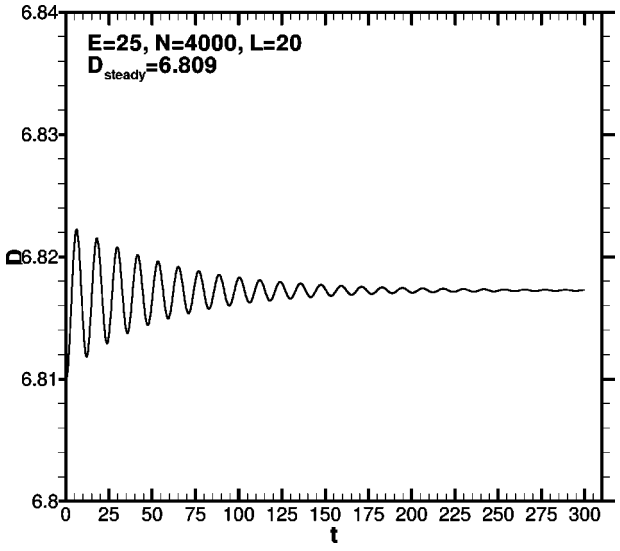

FIG. 7. Stable detonation with $E=25$; $N=4000$ points on the domain of length $L=20$, $N_{1/2}=200$.

Figure 6(b) shows the density profiles after the interaction has occurred. One can see the rarefaction wave and a smeared contact discontinuity propagating to the left away from the lead shock. The effect of the resolution that is more pronounced in this figure can be seen in smearing the contact discontinuity and the rarefaction wave by the spatial discretization scheme.

B. Pulsating detonation with simple-depletion kinetics

In this section, we present several calculations for the development of a detonation wave from an initially prescribed steady Chapman–Jouguet solution. We obtain high-resolution solutions for a stable detonation, weakly unstable detonation with periodic limit cycle, detonation with irregular oscillations, and highly unstable detonation with reignition. We fix the specific heat ratio at $\gamma=1.2$ and the heat release at $Q=50$, and vary the activation energy E similar to that done in, e.g., Refs. 5 and 6. The steady CJ speed for this detonation is $D_{\text{CJ}}=6.809$. The linear stability theory predicts that detonation with these parameters is unstable for $E>E_c=25.26$.

Figure 7 shows the calculated shock speed for detonation below the stability boundary. We used $N=4000$ points on the computational domain of length $L=20$; this gives $N_{1/2}=200$ grid points per half-reaction length. The oscillations are seen to damp out with time as expected. The weakly unstable case of Fig. 8(a) corresponds to $E=26$. The period of the limit cycle solution is $T=12.11$, while the linear stability theory,[8] predicts $T^{\text{LS}}=11.99$. The present resolution predicts the amplitude within a fraction of a percent of that with $N=8000$. The case of an irregular dynamics is shown in Fig. 8(b). For this detonation wave, we have used a higher resolution of $N_{1/2}=400$ due to the stronger dependence of its

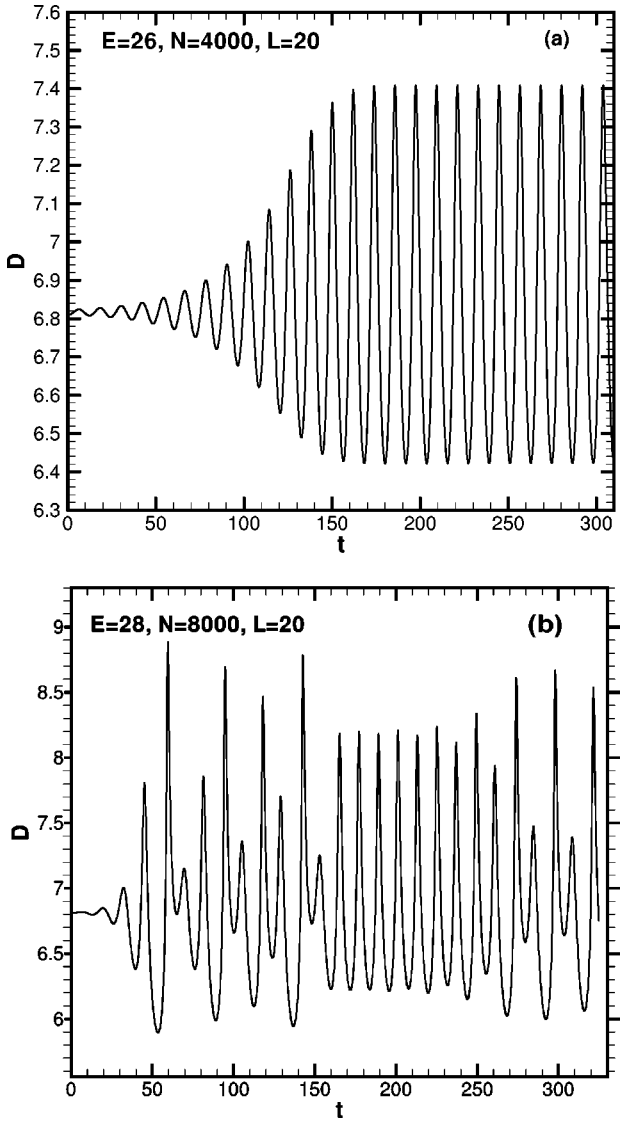

FIG. 8. Weakly unstable detonation with $E=26$, $N=4000$, domain length $L=20$, $N_{1/2}=200$. (b) Irregular detonation with $E=28$, $N=8000$, domain length $L=20$, $N_{1/2}=400$.

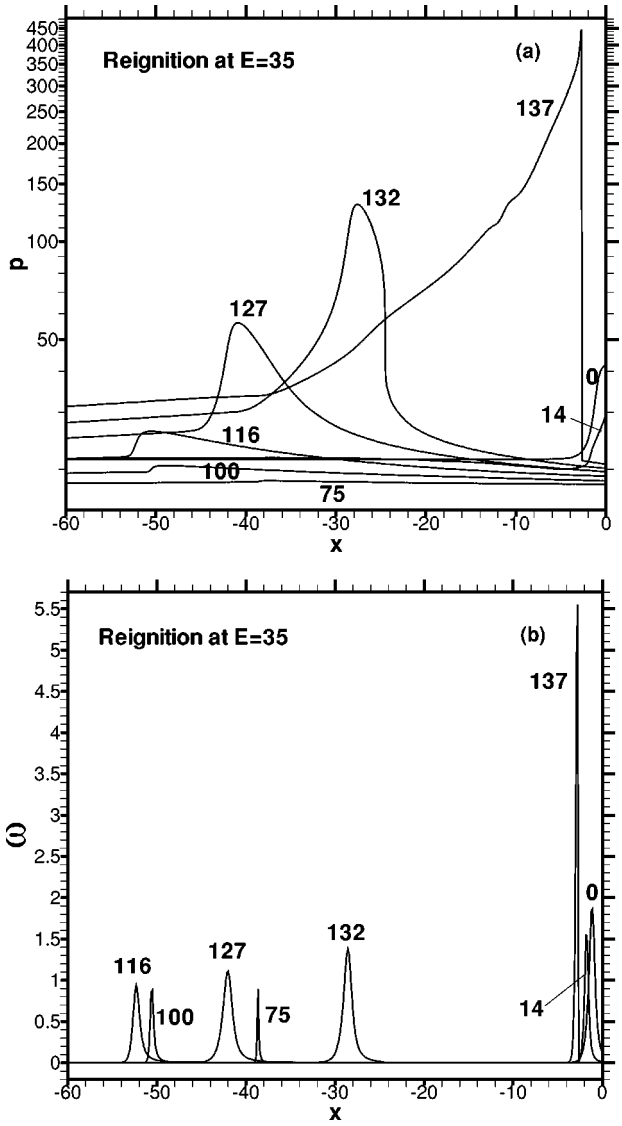

FIG. 9. The sequence of pressure (a) and reaction rate (b) profiles during the reignition $E=35$, $N=16000$, domain length $L=60$, $N_{1/2}=266$. The numbers near the curves indicate corresponding times.

dynamics on the grid size. This is a possible case of a chaotic dynamics understanding of which requires further investigations both numerically and theoretically.

We have also computed the dynamics of a strongly unstable detonation which results in a decay and subsequent reignition of the detonation similar to what has been published in earlier studies.[2,4–6] Figure 9 shows the time-snapshots of the distribution of pressure and reaction rate. The reaction front is seen to detach from the lead shock to a large distance approaching the left end of the computational domain. Eventually, it reverses its direction and starts propagating back toward the shock. In the process, a strong compression wave is generated that develops into a detonation wave overtaking the lead shock front. Figure 10 shows the corresponding speed of the lead shock, the large jump in it corresponding to the moment of overtaking of the lead shock by the internal detonation wave. A similar sequence of events was also found to occur for strongly unstable detonations with chain-branching kinetics in Ref. 17. The reader is referred to Ref. 17 for a more detailed discussion of the underlying mechanisms of such detonations. The computed details of the reignition process are very sensitive to the grid resolution in agreement with previous findings. For example, with low resolution of $N=2000$ ($N_{1/2}=33$) grid points with other parameters the same as in Fig. 9, a series of internal shock waves can be seen to emerge which overtake one another to form a single detonation front in the interior.

With the parameters of Fig. 10, the underlying steady detonation wave is linearly unstable and has two unstable oscillatory modes. The low frequency first mode has a smaller growth rate than the higher-frequency second mode, thus one might expect the high-frequency oscillations to appear first. The phenomenon has in fact been reported by Sharpe and Falle in Ref. 4 which they claim contradicted the original calculations by He and Lee, in that He and Lee's results did not show any early oscillations. Sharpe and Falle attributed the difference to inadequate resolutions used in He and Lee, although both of these works used about 50 grid

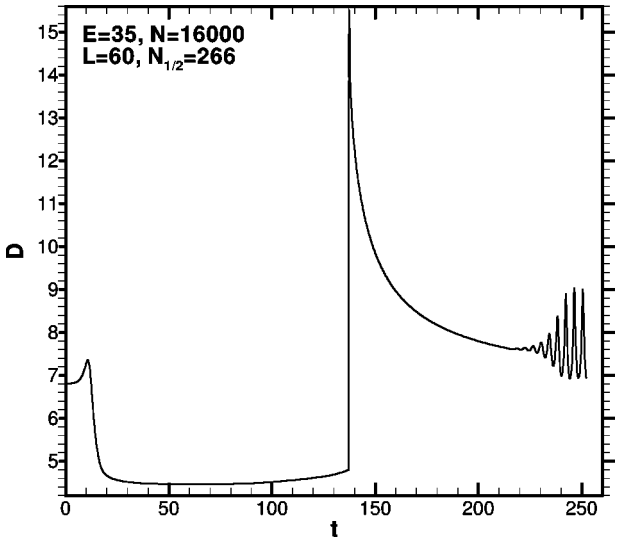

FIG. 10. The shock speed vs time for the strongly unstable case. $E=35$, $N=16000$, domain length $L=60$, $N_{1/2}=266$.

points per half-reaction length. Our calculations, shown in Fig. 10, do not have high-frequency oscillations in agreement with He and Lee, and are computed with higher resolution of 266 points per half-reaction length. We have also carried out calculations using as many as 533 grid points per half-reaction zone and found no early high-frequency oscillations.

The explanation of the absence of oscillations has to do with the initial disturbances to the detonation wave. It is well known that when starting detonation simulations with a steady solution with a discontinuous shock front, one always sees strong overshoots/undershoots in the shock pressure within a few time steps before the discretization scheme smears the shock out. These spurious initial errors are amplified if the underlying detonation structure is unstable. But in our method the shock is always at the origin, therefore there are no significant initial overshoots due to shock-capturing errors. The amplitude of the initial disturbance is so small that the high-frequency instability does not develop before the reaction front decoupling starts. To verify the statement, we computed a case with an artificial initial disturbance introduced by increasing the pressure within five cells adjacent to the shock by $\Delta p=1$, which is about 2.4% of the initial post-shock pressure. Indeed, the growth of this disturbance can be clearly seen in Fig. 11, which corresponds to the same settings as Fig. 10. The period of the oscillations agrees closely with linear stability theory, which predicts that the faster growing second mode of the two unstable modes has a period of $T=1.455$. The oscillations can be seen with initial perturbation of magnitude smaller or larger than the present one. In agreement with previous simulations, higher resolutions tend to make the pulsations persist over longer times, in particular even after the decoupling of the lead shock and reaction front takes place. The oscillations were shown in Ref. 4 to be responsible for the formation of unburnt pockets of gas. Thus we conclude that the absence of the early high-frequency oscillations in Fig. 10 is explained by the absence of the spurious start-up errors near the shock and by dominant low-frequency evolution of the wave. This conclusion is confirmed by Fig. 11(b) which shows very early dynamics of the shock corresponding to Fig. 11(a). It is likely that all shock-capturing schemes suffer from the spurious errors near the shock, which can dramatically affect the flow in the reaction zone and in turn the lead-shock dynamics, especially at large activation energies typical of real mixtures. For example, if the postshock temperature error is at the level of, e.g., 0.1%, and the activation energy scaled with respect to the postshock temperature, T_s, is $E/RT_s=10$, the error in the reaction rate will be 1%. It is the reaction rate, not temperature, that enters the governing equations as a source term, and this large error will dramatically reduce the accuracy of simulations. Shock-tracking methods, on the other hand, can reduce the shock errors significantly and are thus better suited for detonation simulations.

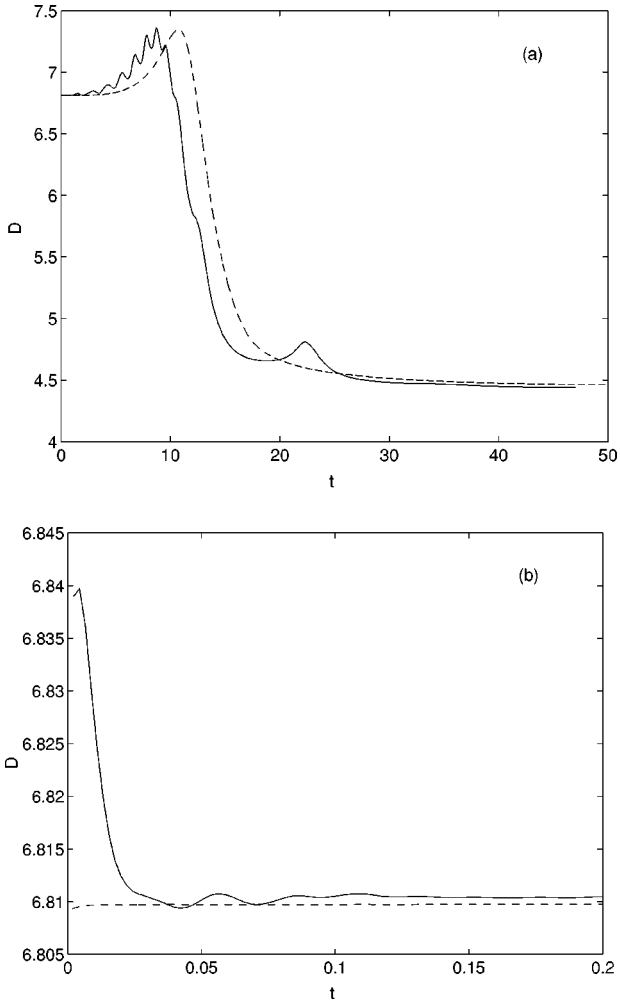

FIG. 11. The early-stage evolution of the strongly unstable detonation: (a) (solid line) and without (dashed line) initial perturbation of the lead shock; (b) zoom into the very early dynamics for the two cases showing no overshoots by the present algorithm (dashed line) and an initial artificial perturbation placed at the shock (solid line).

As to the role of the outflow boundary condition in the cases computed above, it was found to be of minor significance compared to that of a spatial resolution. For the reignition case, the nonreflecting boundary caused a slight delay of the reignition time and a small increase of the maximum

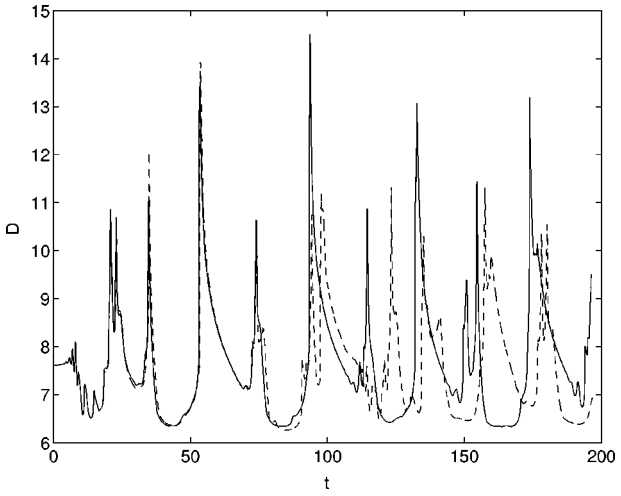

FIG. 12. The shock speed vs time for an overdriven detonation with $Q=E=50$, $\gamma=1.2$, overdrive $f=1.25$: solid line is computed with NRBC, dashed line uses "soft" outflow condition.

shock speed, after the internal detonation wave caught up with the lead shock. The reasons for such a small difference are high resolutions used which tend to reduce the spurious reflections off the boundary and near-sonic character of the flow at the boundary. In simulations of overdriven detonations, in which the subsonic character of the flow behind the shock front allows the reflected waves to catch the front, the nonreflecting boundary condition can play a significant role. As an examp1e, Fig. 12 shows the dynamics of an overdriven detonation with $Q=E=50$, $\gamma=1.2$, and the degree of overdrive $f=1.25$. The computational domain of size $L=40$ has $N=4000$ grid points, which places $N_{1/2}=100$ points within the half-reaction length. The two curves in the figure differ only by the type of the outflow boundary condition used. That the latter has a significant effect on the solution, especially over long times, can be clearly seen.

C. Self-sustained detonation with a finite reaction zone

All calculations above have been carried out for detonation with simple-depletion reaction for which a steady detonation has an infinite length and therefore the sonic locus is located at infinity. One implication of such kinetics for numerical calculations is that no matter how long a computational domain is, the finite size of the domain can eventually influence the computation of the detonation dynamics.

Next we consider an evolution of a detonation wave that starts from a steady CJ solution with a finite reaction zone. In such detonations the domain of influence of the detonation shock is the finite region between the shock and the sonic locus. For unsteady detonations, the Mach number defined in terms of the particle velocity relative to the lead shock does not have the same significance as in steady detonations. Instead, the present interpretation of the sonic locus as an information boundary is something that retains its significance, in which case the unsteady sonic locus must be defined in terms of characteristics. Specifically, we define the sonic locus as a separatrix of forward characteristic lines that remains at a finite nonvanishing distance from the shock at all times. All forward characteristics ahead of the separatrix between the shock and the separatrix will reach the front in finite time, while those characteristics downstream the separatrix will never reach the shock.

Such a definition can be given precisely mathematically as a boundary condition since the separatrix belongs to the family of forward characteristics. Two conditions must be satisfied at the sonic locus:

$$\frac{dx_*}{dt} = c_* + U_* \tag{21}$$

and

$$\frac{dp_*}{dt} + \rho_* c_* \left(\frac{dU_*}{dt} + \frac{dD}{dt} \right) = (\gamma - 1) Q \rho_* \omega_*, \tag{22}$$

where subscript * denotes the sonic state and time derivative is taken along the separatrix in (x,t) plane. Equations (21) and (22) are, of course, the governing equations for forward characteristics and therefore hold for any such characteristics. In fact, any forward characteristic can be considered an information boundary, but the separatrix is the only one that can be such a boundary for all time and always at a finite distance from the shock. If for example, one takes a characteristic which is ahead of the separatrix, one would be able to use it as a boundary condition only for a finite time, before the characteristic hits the shock. If on the other hand, one takes a characteristic behind the separatrix, one would have to deal with increasingly larger computational domain. The special initial condition, namely $c_*(0)+U_*(0)=0$ at $x=x_{*0}$, defines the separatrix.

The existence of an information boundary (i.e., a trailing sonic locus) identifies that detonation wave is self-sustained because the locus is a boundary such that all of the information needed to determine the subsequent motion of the lead shock originates between the lead shock and that boundary. The reaction zone powering the shock is acoustically isolated from the flow trailing this locus. The following calculations were carried out for a detonation wave that has an embedded sonic locus. The same ideal-gas equation of state with $\gamma=1.2$ and $Q=50$ is used, but now the reaction order is taken to be $\nu=0.9$. Since the reaction zone is now finite, the initial state behind the reaction zone can be chosen essentially arbitrarily. In order to understand the role played by the flow behind the steady sonic locus, we compute the unsteady dynamics for two different initial profiles. In the first case, the state behind the sonic point is uniform and the same as the sonic state. For the second case, we put a strong rarefaction wave behind the sonic point. We compute the evolution of the wave at activation energy of $E=26.2$. At these parameters the detonation dynamics is that of a low-frequency pulsation.

In order to illustrate the character of the sonic locus we track the paths of a range of forward characteristic lines that emanate from the neighborhood of the initial sonic locus, which is located at $x_*(0)=-7.92$. Some of the characteristics have their origin in between the steady sonic locus and the shock and, as Fig. 13 shows, they reach the front in finite time. As for the remainder of the characteristic lines, they

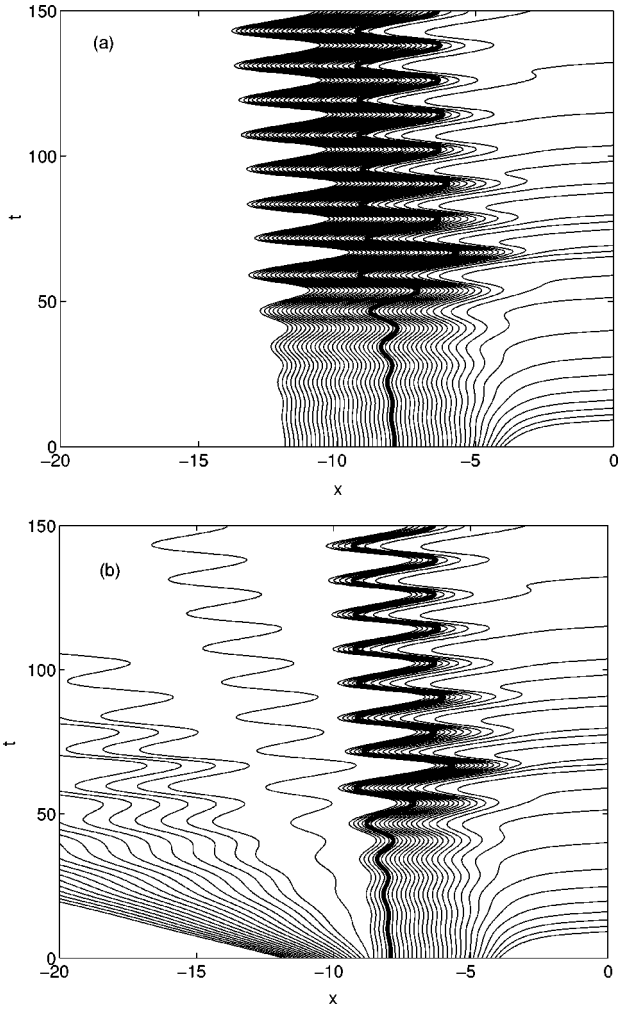

FIG. 13. Characteristic lines emanating from the neighborhood of the steady sonic locus with: (a) uniform initial postsonic state and (b) with a rarefaction wave initially present behind the sonic locus, for detonation with $\gamma=1.2$, $Q=50$, $E=26.2$, and $\nu=0.9$. Thick line in each figure is the separatrix of the characteristics.

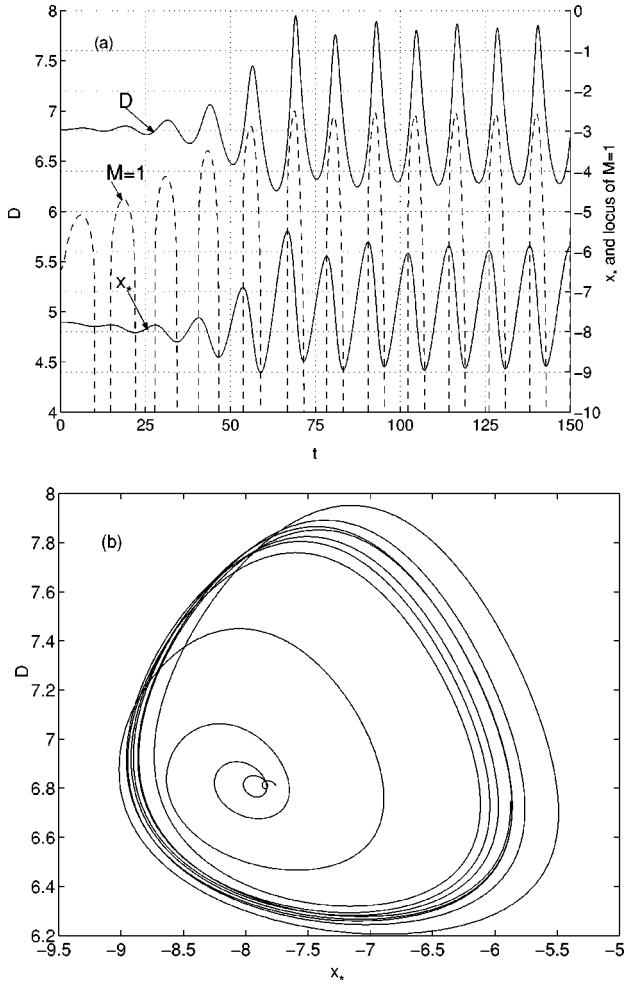

FIG. 14. (a) Shock speed, D, position of the sonic locus, x_*, and the locus of $M=-U/c=1$ as functions of time. (b) The phase plane (D,x_*). All parameters and the initial condition are the same as in Fig. 13(a).

tend to infinity, which means that, on average all forward waves that propagate along these characteristics retreat from the reaction zone. But there exists a *separatrix* of the characteristic lines, which itself is a characteristic, that remains at a finite nonzero distance from the front at all times.

Figure 13 shows that although the flow behind the separatrix is quite different in cases (a) and (b), the flow ahead of it is unchanged. This is consistent with the fact that the domain of influence of the region ahead of the separatrix is between the shock and the initial sonic locus. Consequently, as the front evolves, the domain of influence of the shock front is bounded by the shock and the separatrix. The flow behind the separatrix has no influence on the continuous dynamics of the flow ahead of the separatrix and on the motion of the shock front. Thus, the detonation wave can be looked at as a two-front phenomenon with two free boundaries, namely the shock and the sonic locus.

It must be pointed out, that the Mach number, $M=-U/c$, defined in terms of the particle speed relative to the shock, U, and the local sound speed, c [the locus of $M=1$, corresponding to Fig. 13(a), is shown by the dashed line in Fig. 14(a)] has no special significance in unsteady detonation. Of course, in the limit of a steady detonation, the sonic locus defined in terms of the characteristics coincides with the locus of $M=1$. Figure 14(a) also shows the shock speed and the location of the sonic locus as functions of time. An important point to make is that Dt and $\chi_*(t)$ in Fig. 14 are exactly the same for both cases shown in Fig. 13, which are solutions with different postsonic initial states. This serves to illustrate the fact that the postsonic flow has no influence on neither the shock dynamics nor the motion of the sonic locus. Thus the shock dynamics is determined entirely by the finite region between the shock and the sonic locus as well as an information supplied by the Rankine–Hugoniot conditions. Figure 15 illustrates that the sonic locus enters and leaves the reaction zone during pulsations. In particular, during the shock acceleration phase, the sonic locus is within the reaction zone, hence $1-\lambda_*\neq 0$, while during the shock deceleration phase, the sonic locus is within the burnt products so that $1-\lambda_*=0$.

The above discussion implicitly assumes that a sonic locus that was present in the initial steady solution remains in the flow during subsequent evolution of the detonation. In fact, it may not always be true that an initially present sonic

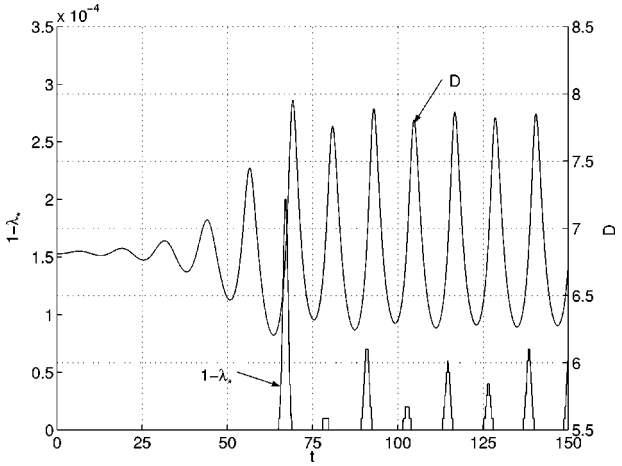

FIG. 15. Shock speed, D, and the reaction-progress variable at the sonic locus, λ_*, as functions of time for the same case as in Fig. 14.

locus will exist for all time. This is true if the flow in the neighborhood of the sonic locus is continuous. But if a shock wave is generated by some mechanism (on either side of the separatrix) that interacts with the sonic locus, then the separatrix will be destroyed. The information carried along the characteristic lines will now be cut by the shock wave and the premise underlying the previous scenario will no longer be true. A smoothly evolving reaction zone is necessary for the information boundary to exist.

The phase plane of D vs x_* is shown Fig. 14(b), in which one can see the characteristic limit cycle behavior with the attractor of a triangular shape. As the strong pulsations of the detonation wave set on, the dynamics of the sonic locus tends to be coupled to that of the shock front as follows. Within one cycle, we see that as the detonation wave decelerates from its steady state speed, the sonic locus starts to move toward the shock from its farthest position of about $x=-9$. As the sonic locus approaches the shock, the shock starts to accelerate which causes the sonic locus to reverse its direction at about $x=-5.5$. As the shock speed reaches the maximum, the sonic locus passes its steady position, $x=-7.92$. After that the shock decelerates and the sonic locus reaches its minimum at $x=-9$. The cycle is repeated. As we can see, the shock deceleration causes the sonic locus approach the shock, where the approach is fastest at the lowest shock speed. Subsequently the shock starts to accelerate with fastest acceleration when the sonic locus is near the shock and then causes the sonic locus to retreat.

That the sonic locus in unsteady detonations defined by Eqs. (21) and (22) have important implications for theories of detonation stability and nonlinear dynamics can be seen by comparing the equations to conditions of linear stability theory, e.g., Ref. 8, and sonic conditions of detonation dynamics, e.g., Ref. 9. The fact that a linearized version of Eq. (22) reduces exactly to the radiation of Lee and Stewart,[8] has its roots in the basic physics of the condition. Both conditions express the same notion of acoustic isolation of the reaction zone from the following flow. Equation (22) holds under much more general conditions, of course, but expresses the same physics as the radiation condition. In fact we note that he radiation condition of Lee and Stewart is actually more general than a derivation of it given Ref. 8 would imply, because it can be obtained directly from the compatibility condition, which is exact, by simple linearization. Comparison to the sonic conditions of the detonation shock dynamics shows that Eq. (22) reduces to what is called a thermicity condition in an appropriate limit of slow evolution.

VI. CONCLUSIONS

In this work we have discussed a role played by the far-field flow in self-sustained one-dimensional detonation waves. If such detonations are steady, then a sonic locus is present at the end of the reaction zone. For detonations that have a finite reaction zone, the sonic locus will also be at a finite location from the lead shock. One of the most important properties of a sonic locus in steady detonations is that the reaction zone is separated by the locus from the influence of the flow behind it. We have generalized the concept of a sonic locus to unsteady detonations and have shown that it is also defined as a separatrix of forward characteristics but which are now unsteady. By means of a new and highly accurate numerical algorithm for the integration of the reactive Euler equations in a frame of reference attached to the lead shock front, we have shown that the separatrix exists and serves as an information boundary that isolates the lead shock from the influence of the far-field flow. We have defined the sonic locus mathematically and have shown that it is a generalization of the radiation conditions of linear stability theory and sonic conditions of detonation shock dynamics. That is, the definition that we have introduced holds for essentially arbitrary detonations (nonlinear and not necessarily slowly-evolving) with the only assumptions that the sonic locus be present and the flow evolution be smooth. Although in this work we restrict ourselves to one-dimensional planar detonations with one-step Arrhenius kinetics and an ideal-gas equation of state, a quite general theory of the sonic conditions can be formulated that holds for three-dimensional detonations with arbitrary equation of state and complex kinetics (details be found in Ref. 18).

The numerical method of calculating detonations in the shock-attached frame can be conveniently used for the purpose of comparison with analytical results which are often done in a shock-attached frame. We have also introduced a nonreflecting boundary condition that significantly reduces the effects of the spurious reflections of waves off the far-field numerical boundary. And finally, we emphasize that the numerical method we propose can be implemented as an extension to any existing numerical scheme. Such an extension makes computations of the shock dynamics much more accurate and affordable and allows for a simple analysis of the physical processes within the reaction zone.

ACKNOWLEDGMENTS

This work was financially supported by the U.S. Air Force Office of Scientific Research under Contracts No. F49620-00-1-0005 and No. F49620-03-l-0048, Program Manager Dr. Arje Nachman. Additional support was pro-

vided by the U.S. Air Force Research Laboratory Munitions Directorate, Eglin AFB, under Contract No. F8630-00-1-0002. D.S.S. was also supported by U.S. Department of Energy, Los Alamos National Laboratory, No. DOE/LANL 3223501019Z.

[1] A. Bourlioux, A. J. Majda, and V. Roytburd, "Theoretical and numerical structure for unstable one-dimensional detonation," SIAM (Soc. Ind. Appl. Math.) J. Appl. Math. **51**, 303 (1991).
[2] D. N. Williams, L. Bauwens, and E. S. Oran, "A numerical study of the mechanisms of self-reignition in low-overdrive detonations," Shock Waves **6**, 93 (1996).
[3] P. Hwang, R. P. Fedkiw, B. Merriman, T. D. Aslam, A. R. Karagozian, and S. J. Osher, "Numerical resolution of pulsating detonation waves," Combust. Theory Modell. **4**, 217 (2000).
[4] G. J. Shape and S. A. E. G. Falle, "One-dimensional numerical simulations of idealized detonations," Proc. R. Soc. London, Ser. A **455**, 1203 (1999).
[5] G. J. Sharpe and S. A. E. G. Falle, "Numerical simulations of pulsating detonations: I. Nonlinear stability of steady detonations," Combust. Theory Modell. **4**, 557 (2000).
[6] L. He and J. H. S. Lee, "The dynamical limit of one-dimensional detonations," Phys. Fluids **7**, 1151 (1995).
[7] J. Erpenbeck, "Stability of steady-state equilibrium detonations," Phys. Fluids **5**, 604 (1962).
[8] H. I. Lee and D. S. Stewart, "Calculation of linear detonation instability One-dimensional instability of plane detonation," J. Fluid Mech. **212**, 103 (1990).
[9] D. S. Stewart, "The shock dynamics of multidimensional condensed and gas-phase detonations," Proc. Combust. Inst. **27**, 2189 (1998).
[10] I.-L. Chen, J. Glimm, O. McBryan, B. Plohr, and S. Yaniv, "Front tracking for gas dynamics," J. Comput. Phys. **62**, 83 (1986).
[11] A. Harten and S. Osher, "Uniformly high order accurate nonoscillatory schemes. I," SIAM (Soc. Ind. Appl. Math.) J. Numer. Anal. **24**, 279 (1987).
[12] S. Xu, T. Aslam, and D. S. Stewart, "High-resolution numerical simulation of ideal and nonideal compressible reacting flows with embedded internal boundaries," Combust. Theory Modell. **1**, 113 (1997).
[13] K. W. Thompson, "Time dependent boundary conditions for hyperbolic systems," J. Comput. Phys. **68**, 1 (1987).
[14] T. J. Poinsot and S. K. Lele, "Boundary conditions for direct numerical simulations of compressible viscous flows," J. Comput. Phys. **101**, 104 (1992).
[15] J. von Neumann, "Progress report on the theory of shock waves," National Defense Research Committee, Division 8, Office of Scientific Research and Development No. 1140 (1943).
[16] B. L. Rozhdestvenskii and N. N. Janenko, "Systemy kvazilineinykh uravnenii i ikh prilozheniya k gazovoi dinamike," 2-e izdanie, Moskva, Nauka, 1978 (Translation: "Systems of quasilinear equations and their applications to gas dynamics," Translations of Mathematical Monographs, Vol. 55, 1983).
[17] M. Short, A. K. Kapila, and J. J. Quirk, "The chemical-gas dynamic mechanisms of pulsating detonation wave instability," Philos. Trans. R. Soc. London, Ser. A **357**, 3621 (1999).
[18] A. R. Kasimov, "Theory of instability and nonlinear evolution of self-sustained detonation waves," Ph.D. dissertation, Department of Theoretical and Applied Mechanics, University of Illinois at Urbana-Champaign, Urbana, Illinois, 2004.